

Bayesian structural learning of microbiota systems from count metagenomic data

Veronica Vinciotti*

Department of Mathematics, University of Trento

and

Pariya Behrouzi*

Department of Mathematics, Wageningen University

and

Reza Mohammadi

Faculty of Economics and Business, University of Amsterdam

Abstract

Metagenomics combined with high-resolution sequencing techniques have enabled researchers to study the genomes of entire microbial communities. Unraveling interactions between these communities is of vital importance to understand how microbes influence human health and disease. However, learning these interactions from microbiome data is challenging, due to the high dimensionality, discreteness, broad dispersion levels, compositionality and excess of zero counts that characterize these data. In this paper, we develop a copula graphical model for structure learning in these settings. In particular, we advocate the use of discrete Weibull regression for linking the marginal distributions to external covariates, which are often available in genomic studies but rarely used for network inference, coupled with a Gaussian copula to model the joint distribution of the counts. An efficient Bayesian procedure for structural learning is implemented in the R package **BDgraph** and returns inference of the marginals and of the dependency structure, providing simultaneous differential analysis and graph uncertainty estimates. A simulation study and a real data analysis of microbiome data show the usefulness of the proposed approach at inferring networks from high-dimensional count data in general, and its relevance in the context of microbiota data analyses in particular.

Keywords: Copula graphical models, discrete Weibull, microbiome, metagenomics

*These authors contributed equally to this work.

1 Introduction

Interactions between microbes are fundamental in shaping the structure and functioning of the human microbiota, and their malfunctioning has been linked to a number of medical conditions. However, a lack of understanding of how these interactions shape and evolve makes it difficult to predict their relevance in biomedical fields. For these reasons, microbiota systems have been intensively studied in recent years. Large consortia have developed technologies for the collection of high-throughput data of the microbiome, e.g., the Human Microbiome Project (HMP Consortium, 2012) and the Metagenomics of the Human Intestinal Tract (MetaHIT) project (Qin et al., 2010). These have paved the way for further studies investigating the association of the microbiota functioning with a number of medical conditions, such as obesity (Le Chatelier et al., 2013) and diabetes (Pedersen et al., 2016), as well as with the response to certain treatments, such as immunotherapy (Lee et al., 2022).

The task of learning these interactions from multivariate data falls in the remit of graphical modelling. Among the approaches available, Gaussian graphical models are by far the most popular, thanks also to their efficient implementations for high dimensional problems (Friedman et al., 2008; Mohammadi and Wit, 2015). Microbiome data are however far from Gaussian, with marginal distributions that are in most cases skewed and with a large mass at zero. For this reason, transformations, such as the logarithm or the centered log ratio, are typically applied to the data, followed by Gaussian graphical modelling approaches on the transformed data. This is for example the case of the two most used methods for microbiome data, SparCC (Friedman and Alm, 2012) and SPIEC-EASI (Kurtz et al., 2015), with recent extensions proposing the incorporation of a zero inflated component to the model (Prost et al., 2021).

The transformations above require a pseudo-count adjustment to be able to handle zeros and may also impact the network inference conducted downstream. In the statistical literature, extensions of Gaussian graphical models to non-Gaussian data can take different forms but there is generally little research for the case of unbounded count data, such as the microbiome data. Roy and Dunson (2020) have recently proposed a pairwise Markov random field model with flexible node potentials, while Cougoul et al. (2019) have proposed a Gaussian copula graphical model with zero-inflated negative binomial marginals, specifically thought for the inference of microbiota systems. Our work is linked to this second paper. Indeed, on the one hand the use of a Gaussian copula facilitates the integration of novel approaches with existing ones that rely on Gaussianity, without the need of ad-hoc transformations. On the other hand, the use of parametric marginal distributions, rather than the non-parametric empirical distributions as in the popular non-paranormal approach (Liu et al., 2009), facilitates the task of incorporating in the model additional covariates, which are often present in genomic studies. Moreover, parametric models allow to account for specific features of microbiota data, such as its sparsity and compositional nature.

In this paper, we advocate the use of discrete Weibull regression for modelling the marginal distributions and linking these to external covariates (Klakattawi et al., 2018; Haselimashhadi et al., 2018; Peluso et al., 2019). The simplicity of this distribution (a two-parameter distribution), coupled with the fact that one parameter is directly related to the probability of zeros and that the two parameters can jointly capture broad levels

of dispersion (from under to over), makes it quite an appealing candidate for the high dimensional and sparse microbiota data, and in general for multivariate count data with a high number of random variables and/or external covariates. Indeed, firstly, for a large number of count variables, one wants to avoid tuning the type of distribution for each variable, and, secondly, for a large number of external covariates, a global requirement of over dispersion at all levels of the covariates could prove too restrictive. Finally, an interesting feature of the discrete Weibull distribution, in the context of Gaussian copula graphical models, is the fact that it is generated as a discretized form of a continuous Weibull distribution. This creates a latent non-Gaussian space in the vicinity of the data, with a one-to-one mapping with the latent Gaussian data, where the conditional independence graph (the network of interactions) resides.

A fundamental problem of copula graphical models for discrete data, bounded or unbounded, is the fact that the marginal distributions are not strictly monotonic. In this setting, while the existence of a copula can still be guaranteed by Sklar’s theorem (Sklar, 1959), its uniqueness can not, leading to potential biases in the inferential procedure. On the one hand, this problem can be alleviated with the use of covariate dependent marginals, particularly when the covariates are continuous and the underlying network does not depend on the covariates (Yang et al., 2020). This can be seen as a second advantage of incorporating covariates in the inference of microbiota systems, beyond the primary interest of estimating their effect on the microbial abundances, as studied for example in Lee et al. (2020). On the other hand, more advanced inferential procedures are required, that account for the fact that each observed count is associated with an interval in the latent Gaussian space. This relies on the ideas of extended rank likelihood (Hoff, 2007) and has been used also in the context of Gaussian copula graphical models, both in a frequentist Expected Maximisation (EM) setting (Behrouzi and Wit, 2019) and in a Bayesian setting (Mohammadi et al., 2017).

While the extended rank likelihood approaches above have been developed for ordinal (bounded) data, their extension to unbounded count data in a parametric setting is relatively simple and will be explored in this paper. The use of these approaches avoids the need for more ad-hoc procedures that condense each interval into one point, with choices such as the right-most point of the interval (essentially using the non-paranormal approach of Liu et al. (2009) on count data) or the point corresponding to the median of the distribution function at the two extremes of the interval as done in Cougoul et al. (2019). These choices, while efficient, may not work well with skewed distributions, or generally distribution functions that are highly stepwise. In this paper, we will develop a Bayesian procedure for structural learning under an expected rank likelihood approach, extending the efficient computational approach that has been recently proposed by Mohammadi et al. (2021). Appropriate choices of a prior distribution on the graphs can be made to encourage sparsity, similar to the frequentist regularized inferential procedures. Importantly, uncertainty on the graph learning can be fully quantified by the procedure, essentially providing a (posterior) probability for each edge. This has not been done before in the analysis of microbiota systems, but plays a crucial role, particularly in high dimensional settings.

In conclusion, this paper presents a novel methodology for the inference of microbiota systems from high dimensional metagenomic count data, characterized by broad dispersion levels, compositionality and excess of zero counts. The key ingredients of this approach are: firstly, discrete Weibull regressions for modelling the marginal distributions and linking

those to external covariates and, secondly, an efficient Bayesian inferential procedure to estimate both the marginal distributions and the underlying graph. This joint procedure will return posterior estimation of the marginals, and possible effects of interest from the covariates, together with the estimation of the graph structure (presence/absence of an edge) and intensity of the interactions. Section 2 will describe the details of the methodology proposed, whose implementation has been included in the R package **BDgraph** (Mohammadi and Wit, 2019). A simulation study in Section 3 and a real data analysis of microbiome data from the HMP in Section 4 will show the usefulness of the proposed approach at inferring networks from high-dimensional count data in general, and in the context of microbiota data analyses in particular. Finally, Section 5 will draw some conclusions and point to future research directions.

2 Methods

In this section, we present the technical details of the proposed method, starting with the definition of a Gaussian copula graphical model and of the discrete Weibull (DW) regression used for the marginal components, followed by the Bayesian inferential procedure.

2.1 Gaussian copula graphical model with DW marginals

Let $\mathbf{Y} = (Y_1, \dots, Y_p)$ be a vector of count variables. In the case of microbiota systems, these are abundances of the individual microbes or, more commonly, of the Operating Taxonomic Units (OTUs) into which they are clustered, e.g. bacterial species. Let F_j , $j = 1, \dots, p$, be the distribution functions associated to the p variables, respectively. In a copula graphical model, the joint distribution of the variables is described via a copula function C that couples, as indeed the denomination copula suggests, the marginal distributions F_j into their joint dependency. Formally:

$$P(Y_1 \leq y_1, \dots, Y_p \leq y_p) = C(F_1(y_1), \dots, F_p(y_p) \mid \Theta),$$

where Θ are the parameters describing the copula function C . In the case of a Gaussian copula (Mohammadi et al., 2017)

$$P(Y_1 \leq y_1, \dots, Y_p \leq y_p) = \Phi_p(\Phi^{-1}(F_1(y_1)), \dots, \Phi^{-1}(F_p(y_p)) \mid \mathbf{R})$$

where Φ_p is the cumulative distribution function of a p -dimensional multivariate normal with a zero mean vector and correlation matrix \mathbf{R} , while Φ is the standard univariate normal distribution function. The dependency structure is captured by the inverse of the correlation matrix $\mathbf{K} = \mathbf{R}^{-1}$, typically called the precision or concentration matrix. Indeed, the zero patterns in this matrix define the conditional independence graph in the latent Gaussian space, following from the theory of Gaussian graphical models (Lauritzen, 1996).

In the context of copula graphical models, the marginal distributions F_j are typically considered as nuisance parameters and estimated by their empirical counterpart. However, as explained in the introduction, external covariates are often available in genomic studies and there is an interest in estimating their effect on the outcome while accounting for the multivariate nature of the data. Moreover, the inclusion of covariates in the marginal components of a copula graphical model on discrete data facilitates the recovery

of the underlying dependency structure. In this paper, we propose to model the marginal components, and their link with covariates, via a discrete Weibull regression (Peluso et al., 2019). Formally, let $\mathbf{X} = (1, X_1, \dots, X_q)$ be a vector of covariates. Then, the conditional distribution of Y_j given \mathbf{X} is modelled by:

$$F_j(y_j|\mathbf{X} = \mathbf{x}) = 1 - q_j(\mathbf{x})^{(y_j+1)^{\beta_j(\mathbf{x})}}, \quad (1)$$

for $y_j = 0, 1, \dots$ and zero otherwise. As the parameter q of the distribution takes values between 0 and 1, and the parameter β is positive, we will consider the logit and the log links, respectively, though other choices are possible (Haselimashhadi et al., 2018). Thus:

$$\log\left(\frac{q_j(\mathbf{x})}{1 - q_j(\mathbf{x})}\right) = \mathbf{x}^t \boldsymbol{\theta}_j$$

$$\log(\beta_j(\mathbf{x})) = \mathbf{x}^t \boldsymbol{\gamma}_j,$$

with $\boldsymbol{\eta}_j$ and $\boldsymbol{\gamma}_j$ denoting the regression coefficients associated to the Y_j marginal component of the model. The simplest case of only the intercept in each model corresponds to the case of discrete Weibull marginal distributions. A zero-inflated version of the model can also be considered, as in (Burger et al., 2020). As microbiome data are very sparse, the real data analysis will also consider a model with an additional zero inflation parameter π_j , although we find that this zero-inflated model is never selected against the simpler model.

A few properties of a discrete Weibull distribution make it an ideal candidate for modelling high dimensional count data. In particular:

1. $F_j(0|\mathbf{X} = \mathbf{x}) = P(Y_j = 0|\mathbf{X} = \mathbf{x}) = 1 - q_j(\mathbf{x})$, thus the parameter q focuses directly on the proportion of zeros in the data. This may be the reason why in the real application, the zero inflated version of the model is not selected for any of the OTUs.
2. The two parameters of the distribution are sufficient to capture both under and over dispersion levels, while still being a parsimonious choice (e.g. same number of parameters as the commonly used negative Binomial distribution). This has been shown to be useful on real data analyses of count data, particularly in the case of under dispersion (Peluso et al., 2019). Although microbiome data are typically highly over dispersed, the presence of a large number of external covariates could make a global requirement of over dispersion at all levels of the covariates \mathbf{x} too restrictive. Moreover, this property is appealing for the development of a model that is suited for any generic high dimensional multivariate count data, without the need for separate fine tuning of the most appropriate marginal distribution for each variable.
3. The quantiles of the distribution have a closed-form expression. In particular, re-parametrizations that are based on the median are useful when quantification of the covariate effects is of primary interest (Burger et al., 2020).
4. The distribution is developed as a discretized form of the continuous Weibull distribution (Chakraborty, 2015). Namely, defining the cdf of a continuous Weibull distribution by

$$F_{CW}(y; q, \beta) = 1 - \exp\left[-\left(\frac{y}{(-\log q)^{-\frac{1}{\beta}}}\right)^\beta\right], \quad y \geq 0,$$

one can easily show that the probability mass function of the discrete Weibull distribution, associated to the cdf in Equation 1, is given by

$$f(y; q, \beta) = q^{y^\beta} - q^{(y+1)^\beta} = F_{CW}(y+1) - F_{CW}(y) = \int_y^{y+1} f_{CW}(t) dt \quad y = 0, 1, 2, \dots$$

This creates a one to one connection between the latent continuous Weibull space, with the same parameters as the discrete Weibull distribution, and the Gaussian space on which the conditional independence graph resides, as depicted schematically in Figure 1.

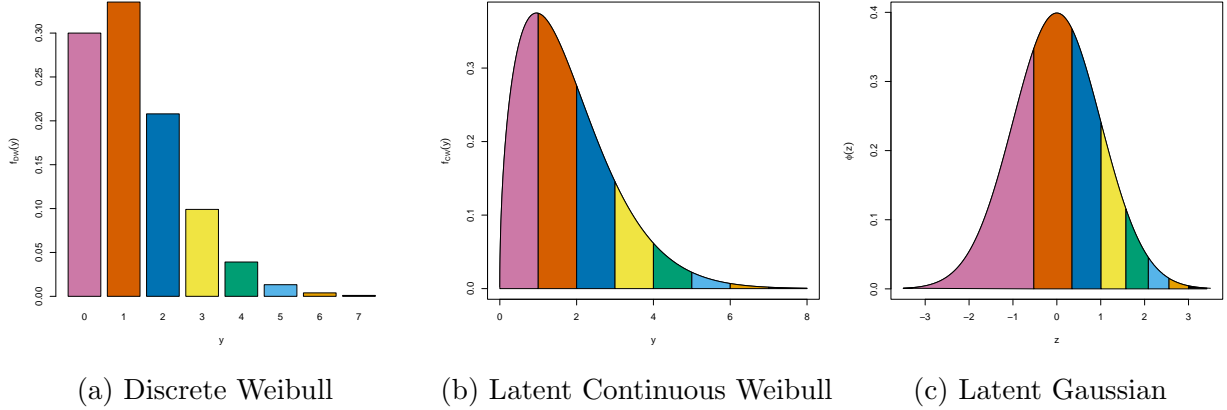


Figure 1: Schematic connection between (a) the discrete Weibull probability mass function $f(y; q = 0.7, \beta = 1.5)$, (b) the underlying continuous Weibull density $f_{CW}(y; q, \beta)$ and (c) the latent Gaussian $z = \Phi^{-1}(F_{CW}(y; q, \beta))$. Each colour relates to the probability associated to the corresponding value of the discrete random variable.

As it is clear also from the figure, each discrete observation is linked to an interval in the continuous spaces. This is indeed the case for copula models on discrete data in general and will require special attention when it comes to inference, as we will discuss more in details in the next section.

2.2 Bayesian inference for a DW graphical model

Inference for copula graphical models involves estimation of the marginals and of the network component. A copula formulation enables us to learn the marginals separately from the dependence structure of the p-variate random variables.

Let us then concentrate on the marginal components first, that is the estimation of the regression coefficients θ_j and γ_j , $j = 1, \dots, p$. Given n observations on component Y_j , denoted with the vector \mathbf{y}_j , and on the q-dimensional vector of covariates, stored in the $n \times q$ matrix \mathbf{x} with \mathbf{x}_i the vector corresponding to the i^{th} row, the likelihood for component

j is given by

$$L_j(\mathbf{y}_j, \mathbf{x} \mid \boldsymbol{\theta}_j, \gamma_j) = \prod_{i=1}^n \left[\left(\frac{e^{\mathbf{x}_i^t \boldsymbol{\theta}_j}}{1 + e^{\mathbf{x}_i^t \boldsymbol{\theta}_j}} \right)^{y_{ij}^{(e^{\mathbf{x}_i^t \boldsymbol{\theta}_j} \gamma_j)}} - \left(\frac{e^{\mathbf{x}_i^t \boldsymbol{\theta}_j}}{1 + e^{\mathbf{x}_i^t \boldsymbol{\theta}_j}} \right)^{(y_{ij}+1)(e^{\mathbf{x}_i^t \boldsymbol{\theta}_j} \gamma_j)} \right],$$

where we consider the logit and log links on the q and β parameters, respectively. Based on this likelihood, we perform inference on the marginal components using an adaptive Metropolis-Hastings scheme, as in (Haselimashhadi et al., 2018). For the simulations and real data analysis in this paper, we set standard Gaussian priors on the regression coefficients $\boldsymbol{\theta}_j$ and γ_j .

Once the marginals are estimated, inference of the network component requires an inverse mapping from the observed to the latent Gaussian space. As noted before, and depicted visually in Figure 1, each observed discrete value corresponds to an interval in the latent Gaussian space with the same associated probability. Formally, z_{ij} can take all the values in the interval $\left(\Phi^{-1}(F_j(y_{ij} - 1)), \Phi^{-1}(F_j(y_{ij})) \right]$, for $i = 1, \dots, n$ and $j = 1, \dots, p$. Thus, given the $n \times p$ data \mathbf{y} and the fitted marginals, the Gaussian latent variables are constrained in the intervals

$$\mathcal{D}_F(\mathbf{y}) = \{ \mathbf{z} \in \mathbb{R}^{n \times p} : \Phi^{-1}(F_j(y_{ij} - 1)) < z_{ij} \leq \Phi^{-1}(F_j(y_{ij})) \}.$$

Rather than condensing these intervals into a single point, as in (Cougoul et al., 2019), we retain this information within the MCMC sampling scheme, similar to the approach of Mohammadi et al. (2017) for ordinal data.

In particular, the extended rank likelihood function for a given graph G and associated precision matrix $\mathbf{K} = \mathbf{R}^{-1}$ is defined as

$$L_E(\mathbf{z} \in \mathcal{D}_F(\mathbf{y}); \mathbf{K}, G) = \int_{\mathcal{D}_F(\mathbf{y})} P(\mathbf{z} \mid \mathbf{K}, G) d\mathbf{z}$$

where $P(\mathbf{z} \mid \mathbf{K}, G)$ is the profile likelihood in the Gaussian latent space:

$$P(\mathbf{z} \mid \mathbf{K}, G) \propto |\mathbf{K}|^{n/2} \exp \left\{ -\frac{1}{2} \text{Trace}(\mathbf{K} \mathbf{U}) \right\}$$

with $\mathbf{U} = \mathbf{z}^t \mathbf{z}$ the sample moment.

The likelihood is combined to priors to lead to the posterior

$$P(\mathbf{K}, G \mid \mathbf{z} \in \mathcal{D}_F(\mathbf{y})) \propto L_E(\mathbf{z} \in \mathcal{D}_F(\mathbf{y}); \mathbf{K}, G) P(\mathbf{K} \mid G) P(G)$$

where $P(\mathbf{K} \mid G)$ denotes the prior distribution on the precision matrix \mathbf{K} for a given graph structure G and $P(G)$ denotes a prior distribution for the graph G . The latter is taken as an Erdős-Rényi random graph with a prior probability of a link $\pi \in (0, 1)$ (which we set to 0.5, representing the case of a noninformative prior, unless stated otherwise), while, conditional on a given graph G , we consider a G-Wishart distribution for the precision matrix \mathbf{K} (Roverato, 2002)

$$P(\mathbf{K} \mid G) = \frac{1}{I_G(b, \mathbf{D})} |\mathbf{K}|^{(b-2)/2} \exp \left\{ -\frac{1}{2} \text{tr}(\mathbf{D} \mathbf{K}) \right\},$$

where $b > 2$ are the degrees of freedom, \mathbf{D} is a symmetric positive definite matrix, and $I_G(b, \mathbf{D})$ is a normalizing constant. For the simulations and real data analysis in this paper, we set a $W_G(3, \mathbb{I}_p)$ prior distribution.

As the space of possible graphs is very large, efficient sampling procedures are needed. In this paper, we use a continuous birth-death MCMC algorithm with efficient calculations of the birth and death rates for adding or removing an edge, respectively, as developed in (Mohammadi et al., 2021). In particular, the algorithm cycles through the following main steps:

1. Sampling the latent data for each marginal j , updating the latent n values \mathbf{z}_j from their full conditional distribution:

$$Z_j | \mathbf{K}, \mathbf{Z}_{V \setminus \{j\}} = \mathbf{z} \sim N\left(-\sum_k \frac{K_{jk} z_k}{K_{jj}}, \frac{1}{K_{jj}}\right)$$

each truncated on its corresponding interval $\mathcal{D}_{F_j}(\mathbf{y}_j)$ with F_j the marginal distribution of component j fitted via a discrete Weibull regression model;

2. Calculating birth and death rates for adding/removing edges as in (Mohammadi et al., 2021):

$$\beta_e(\mathbf{K}) = \min\left\{\frac{P(\mathbf{K}^{+e}, G^{+e} | \mathbf{z} \in \mathcal{D}_F(\mathbf{y}))}{P(\mathbf{K}, G | \mathbf{z} \in \mathcal{D}_F(\mathbf{y}))}, 1\right\}$$

$$\delta_e(\mathbf{K}) = \min\left\{\frac{P(\mathbf{K}^{-e}, G^{-e} | \mathbf{z} \in \mathcal{D}_F(\mathbf{y}))}{P(\mathbf{K}, G | \mathbf{z} \in \mathcal{D}_F(\mathbf{y}))}, 1\right\}$$

3. Sampling the new precision matrix: \mathbf{K}_e^+ or \mathbf{K}_e^- from the G-Wishart posterior.

Following from the Bayesian inference of the Gaussian copula graphical model with discrete Weibull marginals, one can extract any information of interest for the analysis. In particular, from the marginal components, one obtains the posterior distribution of the regression coefficients and can investigate any effect of interest, while from the graph posterior, one can calculate the posterior edge inclusion probabilities:

$$\pi_e = P(e \in E | \mathbf{Y}) = \frac{\sum_{t=1}^N 1(e \in G^{(t)}) W(\mathbf{K}^{(t)})}{\sum_{t=1}^N W(\mathbf{K}^{(t)})}, \quad (2)$$

where E denotes the set of edges, N the MCMC iterations (after burn-in) and $W(\mathbf{K}^{(t)})$ the waiting time for graph $G^{(t)}$ with precision matrix $\mathbf{K}^{(t)}$. These probabilities capture the full uncertainty on the graph learning, which is particularly useful in high dimensional settings such as the microbiome data.

3 Simulation study

The main motivation for the proposed method, inspired by the microbiome analysis, is that of learning the underlying structure of dependency from complex and heterogeneous count data.

In the simulations, we consider two main settings. In the first one, we test the robustness of the proposed method to marginal distributions of different types and compare our approach with other approaches that either treat the marginals as non-parametric (Behrouzi and Wit, 2019; Liu et al., 2009; Mohammadi et al., 2017) or that assume specific parametric forms (Cougoul et al., 2019). In the second setting, we assess the impact of the inclusion of covariates in the marginal component of the model on graph recovery. For all simulations, we consider networks with $p = 10$ nodes, 9 edges (i.e. 20% sparsity) and 3 different types of graph structure: random, scale-free, and clustered with 2 clusters. We evaluate the performance of the methods in terms of the area under the associated Receiver Operating Characteristic (ROC) curve. For our method, this is obtained by setting cutoffs on the posterior edge inclusion probabilities in Equation 2. For frequentist approaches based on penalised inference, we construct the ROC curve across the path of solutions generated by the tuning penalty parameter.

Given a graph G and marginals F_j , $j = 1, \dots, p$, we use the following procedure to simulate count data. We first generate a precision matrix from a G-Wishart distribution, $\mathbf{K} \sim W_G(3, \mathbb{I}_p)$ and standardize it to the inverse of a correlation matrix. We then draw $n = 100$ multivariate normal samples from $N_p(\mathbf{0}, \mathbf{K}^{-1})$. This generates a matrix \mathbf{Z} of dimension $n \times p$. Finally, we obtain the discrete data using $y_{ij} = F_j^{-1}(\Phi(z_{ij}))$, for $i = 1, \dots, n$ and $j = 1, \dots, p$, with Φ the standard normal distribution and F_j a distribution function of a specified shape as explained below.

3.1 Impact of marginal distributions on graph recovery

In the first simulation, we consider the following scenarios for the marginals:

1. DW over-dispersed with q uniformly drawn in (0.6,0.7) and β in (0.4,0.5), i.e. generating dispersion levels between around 40 and 436;
2. DW under-dispersed with q uniformly drawn in (0.85,0.9) and β in (2.5, 3), i.e. dispersion levels between around 0.4 and 0.6;
3. Negative Binomial with μ uniformly drawn in (5, 35) and ϕ in (0.1,0.25), i.e. with mean and variance levels similar to the DW over-dispersed case;
4. Poisson with μ uniformly drawn in (1,2), i.e. with a percentage of zeros between 13.5% and 36.8%, similar to the cases above.

We compare the following 5 methods. Firstly, we consider our own method, a Gaussian copula graphical model with discrete Weibull marginals, that we abbreviate to DWGM. We run the Bayesian inferential procedures for 10k iterations for each marginal and 500k iterations for the structural learning, and set the priors as specified in the description of the method. Secondly, we consider the Bayesian Gaussian copula graphical model (GCGM) for ordinal data of Mohammadi et al. (2017), implemented in the R package **BDgraph**. We use 500k iterations also in this case and the same prior specifications. In the absence of covariates, the Bayesian structural learning procedure of this method is very similar to our approach. Indeed, using non-parametric empirical distribution functions means restricting the distribution to its observed values, but given enough data, this may have little effect on performance. Thirdly, we consider a Gaussian copula graphical model for

ordinal data, where inference is conducted using a frequentist EM-algorithm approach and under a penalized likelihood scheme. This is implemented in the R package `netgwas` (Behrouzi and Wit, 2019). The three approaches above are based on the extended rank likelihood, as described before. We also compare with two approaches that do not use extended rank likelihood. The first one transforms the data using a truncated empirical distribution function (Liu et al., 2009) before using graphical lasso on the transformed data. This is implemented in the R package `huge` and essentially uses the right-bound of the interval for the transformation to the latent Gaussian variable (i.e. $z_{ij} = \Phi^{-1}(F_j(y_{ij}))$). The second one, implemented in the R package `rMAGMA` (Cougoul et al., 2019), uses negative Binomial distributions for the marginals (with a constant dispersion parameter for each marginal and a mean dependent on the covariates) before transforming the data using the mean of the interval, i.e. $z_{ij} = \Phi^{-1}\left(\frac{F_j(y_{ij} - 1) + F_j(y_{ij})}{2}\right)$, and then proceeding with graphical lasso on the transformed data.

Figure 2 shows the performance of DWGM on this simulation, whereby for each graph-marginal combination, we plot the boxplot of the AUC values across 10 simulated graphs of that type and, for each graph, 50 simulated datasets with the marginal distributions of that type. In the simulation, we set the seed in such a way that the same marginal distributions are used across the different graph types, in order to facilitate cross-comparisons. The simulation shows a good performance across the three different graph types, with a slight under-performance for the scale-free graph as found also in other more extensive studies (Cougoul et al., 2019; Prost et al., 2021). Moreover, the simulation shows a robustness of the approach to the miss-specification of the marginal distributions, considering that the six cases on the right of the figure are simulated using marginal distributions that are not those fitted by the model.

Figure 3 presents the results split by marginal distributions but across all graph types, alongside the same information for the other four methods mentioned above. These results show similar performances across the methods and inferential procedures. There is a slight improvement in performance between DWGM and GCGM and the other three methods, even in the case when the alternative methods are correctly specified, namely `rMAGMA` in the case of negative Binomial marginals. Since `netgwas` is a frequentist version of GCGM, we speculate that the improvement comes from a better separation between the presence/absence of links provided by the posterior edge probabilities rather than by edge weights calculated across the penalised path. On the whole, however, as we compare parametric versus non-parametric approaches as well as parametric approaches that are clearly miss-specified, such as `rMAGMA` on DW underdispersed data, we conclude from this simulation that, in the absence of covariates, the parametric choice of the distribution used for the marginals has little impact on network recovery.

3.2 Impact of the inclusion of covariates on graph recovery

In the second simulation setting, we test the performance of the methods when covariates are present in the study and the robustness of approaches that do not include covariates. Of the five methods considered above, we only retain our proposed method (DWGM) and `rMAGMA`, as they are the only ones developed to account for covariates at the marginal level. For this simulation, we consider a random graph with 9 edges (20% sparsity), a

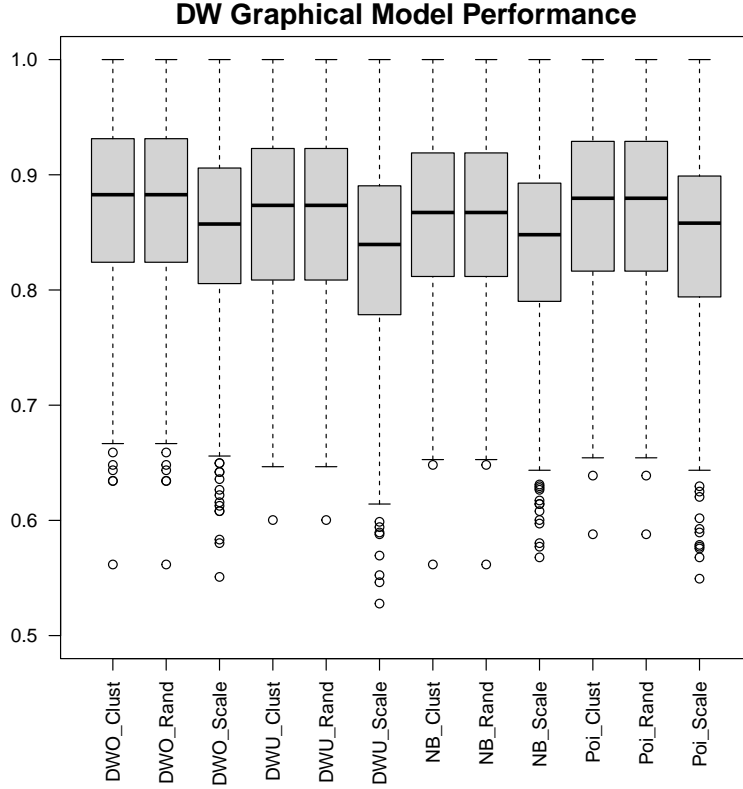


Figure 2: AUC values of network recovery on data simulated with specific marginal distributions, across three different graph types. Each boxplot reports the results from 10 simulated graph structures of the corresponding type and, for each graph, 50 simulated datasets from a Gaussian copula graphical model with the corresponding marginal specifications.

binary external covariate X drawn from a Bernoulli(0.5), e.g. observations split into two groups as in the real data analysis (two environments: stool and saliva) and we simulate marginals in the following three settings:

1. DW under-dispersed with $\log(\beta(x)) = \gamma_0 = \log(2.5)$ (not dependent on X) and $\log(q(x)/(1 - q(x))) = \theta_0 + \theta_1 x$, with $\theta_0 = \log(0.85/(1 - 0.85)) = 1.734$ and three cases for θ_1 capturing increasing levels of dependency from X , namely $\theta_1 \in \{0, 1, 2\}$;
2. DW over-dispersed with $\log(\beta(x)) = \gamma_0 = \log(0.7)$ (not dependent on X) and $\log(q(x)/(1 - q(x))) = \theta_0 + \theta_1 x$, with $\theta_0 = \log(0.5/(1 - 0.5)) = 0$ and $\theta_1 \in \{0, 1, 2\}$;
3. NB with similar mean and variance levels to the previous case across the three settings, namely a constant dispersion parameter $\phi = 0.5$ and $\log(\mu) = \theta_0 + \theta_1 x$, with $\theta_0 = \log(2) = 0.693$ and $\theta_1 \in \{0, 1.2, 2.5\}$.

Figure 4 shows the AUC values for the three settings, across 50 simulated datasets, both for a model that includes covariates in the marginal and a model that does not include covariates, i.e. a model with DW marginals in the case of DWGM and NB marginals in the case of rMAGMA. For DWGM, we run again 10k MCMC iterations for each marginal and

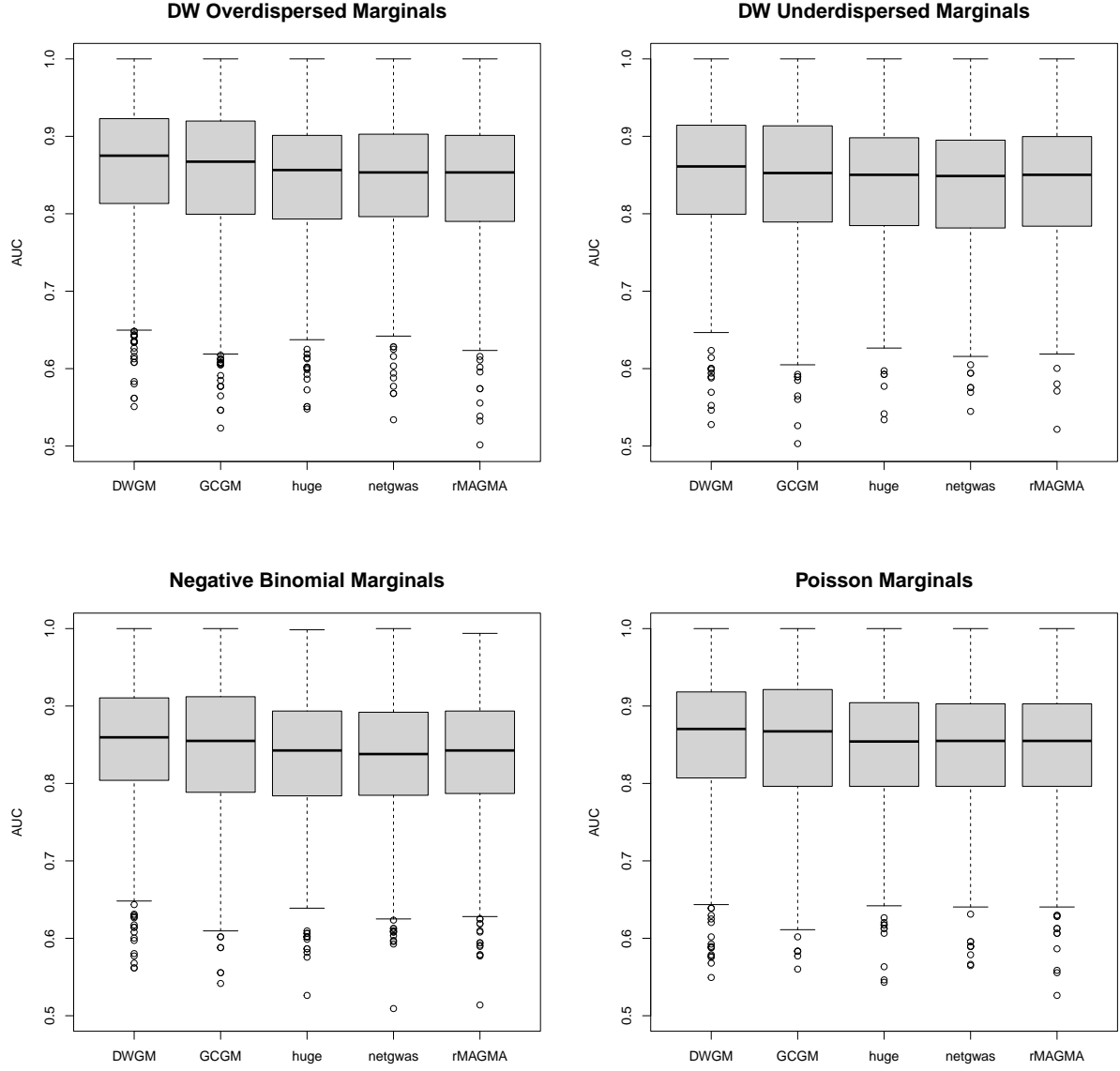


Figure 3: AUC values of network recovery on data simulated with specific marginal distributions across 30 simulated graphs, of type random, scale-free or clustered (10 each). Each boxplot reports the results from the 30 simulated graph structures, and, for each graph, 50 simulated datasets from a Gaussian copula graphical model with the corresponding marginal specifications.

500k for the structural learning. The results show how both methods are performing well when covariates are included in the model, even in the case of miss-specification (namely, rMAGMA on DW marginals and DWGM on NB marginals) supporting the results from the first simulation. Indeed, including the binary covariate corresponds to fitting DW and NB marginals within each of the two groups, thus returning to a case similar to that of the first simulation. However, when covariates are omitted in the models, firstly we notice how the performance of both methods deteriorates as the dependency on the covariates gets

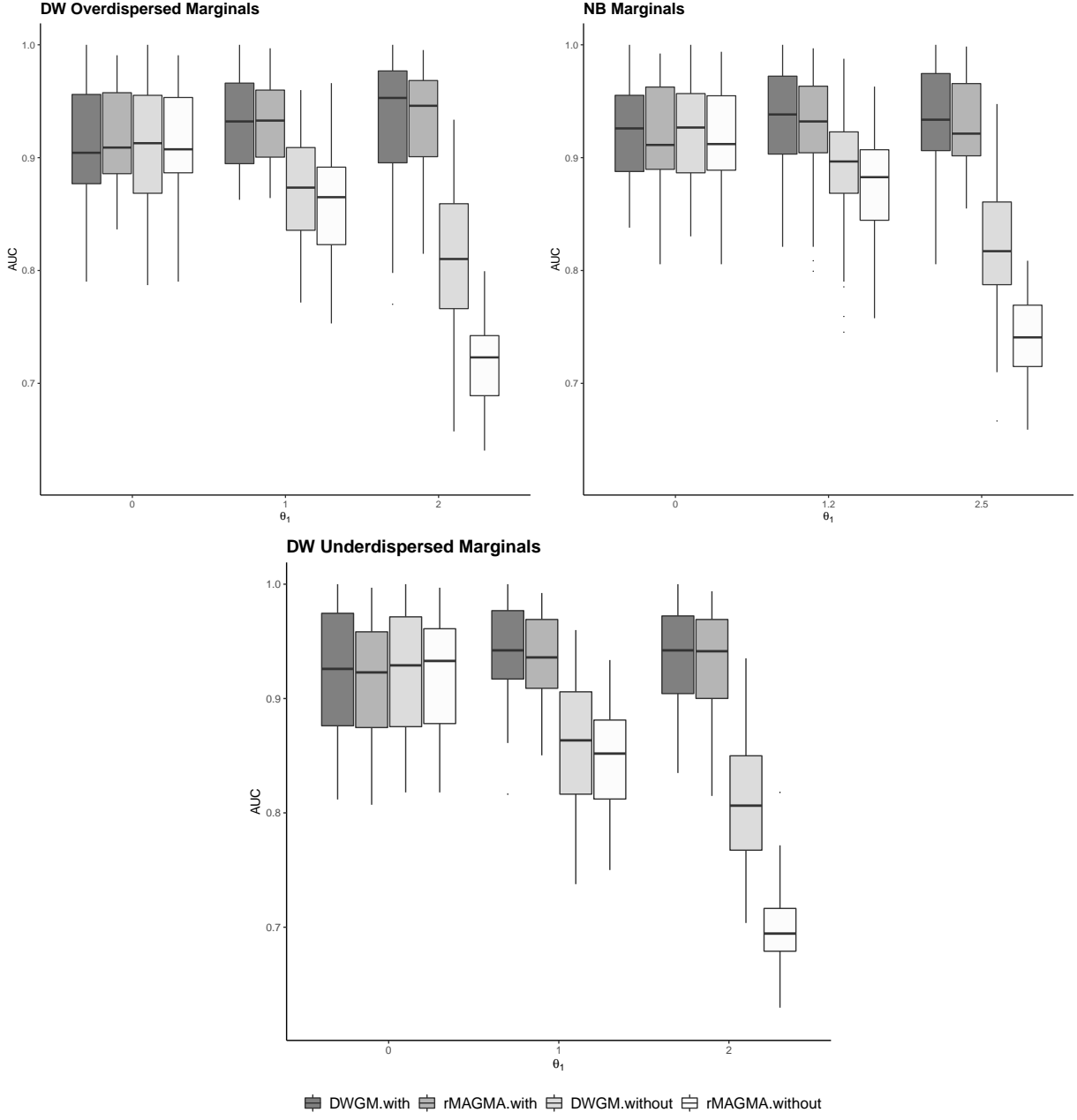


Figure 4: AUC values of network recovery on data simulated with DW and NB marginals linked to a binary covariate X via constant β (for DW) and ϕ (for NB) parameters, but q (for DW) and μ (for NB) parameters dependent on X through a regression coefficient θ_1 . The DWGM and rMAGMA models that account for covariates (DWGM.with and rMAGMA.with, respectively) are compared with the corresponding models with parametric marginals not dependent on X (DWGM.without and MAGMA.without, respectively), across increasing values of θ_1 .

more pronounced. This is indeed the effect of the omission of the covariates, which typically results in the detection of spurious interactions to compensate from the unaccounted differences in means (Vinciotti et al., 2016). Secondly, we notice how rMAGMA is generally

more impacted by this miss-specification than DWGM, with a lower performance at the largest θ_1 value, even in the case of NB marginals in each group. As a binary covariate tends to generate bimodal distributions and/or longer tails, we conclude that DW is more robust to these situations than negative Binomial. Given that many real datasets may have unmeasured covariates or more complex marginal distributions than those implied by DW and NB, we take this as a suggestion to use DWGM for analyses of multivariate count data.

4 Inferring the network of gut microbiota

In this section, we use Gaussian copula graphical models with discrete Weibull marginals to recover the network of interactions between microbial species. As in Cougoul et al. (2019), we retrieve the 16S variable region V3-5 data from the Human Microbiome Project (HMP Consortium, 2012) and perform the analysis at the level of Operating Taxonomic Units (OTUs). We consider 734 microbiomes from healthy individuals and from two different body sites, namely stool and saliva. The data record the abundance of 10730 OTUs, but many are very sparse. With a view to network recovery, we retain the OTUs with more than 2 distinct observed values in both the saliva and stool samples. This leaves us with 386 OTUs, but still a high degree of sparsity, with percentages of zeros per OTU ranging from 40.7% to 99.4%. We further restrict our attention to the 155 OTUs which are present in at least 75% of the samples. These are the nodes of the network. Finally, we remove the samples with less than 500 reads, leaving us with 663 measurements on the 155 OTUs.

The aim is to recover a network of interactions between microbes that is shared by the different environments, while taking into account the fact that the OTU abundances may differ between the different body sites as well as of potential normalizing factors that are often present in genomic data. Indeed, in the case of microbiome data, it is well known how sequencing depths change significantly between samples due to experimental effects. As in Cougoul et al. (2019), we estimate the library size of each sample by the geometric mean of pairwise ratios of OTU abundances of that sample with all other samples.

4.1 Accounting for covariates via DW regression marginals

We use the estimated library size as one covariate in the marginal regression models, together with the body site covariate, indicating whether a sample is from stool or saliva. We fit discrete Weibull marginal models, linking both parameters q and β to the covariates as described previously, i.e. 6 parameters per marginal component. We use 50k MCMC iterations, retaining the last 25% as samples from the posterior distribution. As the data are very sparse, we fit also a zero-inflated discrete Weibull distribution, with a constant zero inflation parameter π_j for component j , on which we place a Beta(1,1) prior distribution. Comparing the zero-inflated versus the standard DW regression model using the Bayesian Information Criterion (BIC), we found that no OTU necessitated the zero-inflated component of the model. As a matter of comparison, we also fitted negative Binomial, using its most common formulation with a mean dependent on the covariates and a constant dispersion parameter, as in Cougoul et al. (2019). Here we found that 11 out of the 155 OTUs (so about 7%) were better fitted with a zero-inflated NB model. This, on one hand, shows how using a zero-inflated model upfront because the data are very sparse, as done in

all the literature on microbiome analyses, may not necessarily be the best option and, on the other hand, how discrete Weibull regression is able to reach a good fitting without the need of zero inflation. This may be down to the fact that one parameter of the distribution (q) is solely concentrated on the percentage of zeros, capturing how this percentage may vary with the covariates.

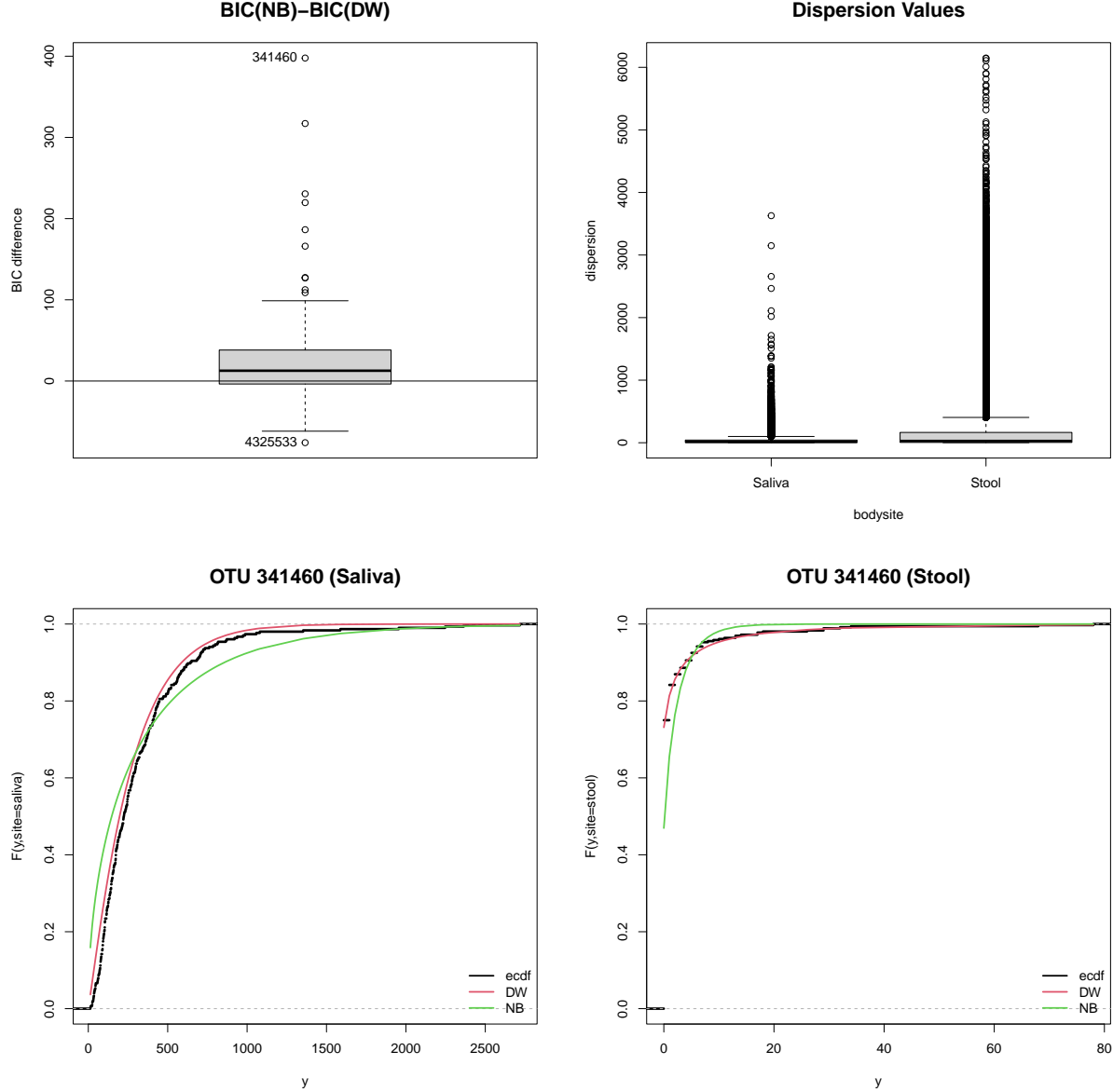


Figure 5: Top: Boxplot of BIC differences between the NB model and the DW model across all 155 OTUs (left) and dispersion levels from the fitted DW model for each OTU and each observation, split by body site (right). Bottom: Cumulative distribution functions (empirical and fitted) corresponding to each body site for the OTU where the BIC difference is largest (397.7402).

Figure 5 shows how a discrete Weibull regression model has, for most OTUs, a lower BIC than a negative Binomial regression model (where we consider here the BIC of the

best model between the zero-inflated and the non-zero inflated version), with various cases showing a significantly better fit for DW. In the right plot, we calculate the dispersion ratio (i.e. the variance divided by the mean) from the fitted DW marginals for each observation and each OTU. The plot shows how the data are highly over-dispersed in both conditions, a setting where NB is typically the preferred choice. Finally, the bottom plots show the OTU with the largest BIC difference, i.e. the OTU best fitted by DW when compared to NB. Here, we plot the cumulative distribution functions of DW and NB associated to the two body sites, while taking an average of the parameters across the normalizing factor. Superimposing these on the empirical cumulative distribution functions associated to the two groups, we see how discrete Weibull shows a better fit overall, and especially at zero, supporting the considerations above.

Including covariates in the inference of microbiota systems has the advantage that analyses that are typically conducted on a microbe by microbe basis are now naturally embedded in the overall joint model. Indeed, we can inspect the estimation and inference of any marginal effect of interest. In this particular analysis, there is interest in detecting the OTUs that are differentially expressed between the two different body sites. Figure 6 shows how all 155 OTUs differ significantly between the two body sites. Furthermore, the plots show how the regression coefficient of the q parameter is highly significant, suggesting large differences between the proportion of zeros in the two environments for most OTUs. In contrast to this, the regression coefficient of the β parameter is less significant. This may in fact indicate that a simpler DW regression model, with a constant β parameter, may be sufficient for some of the OTUs.

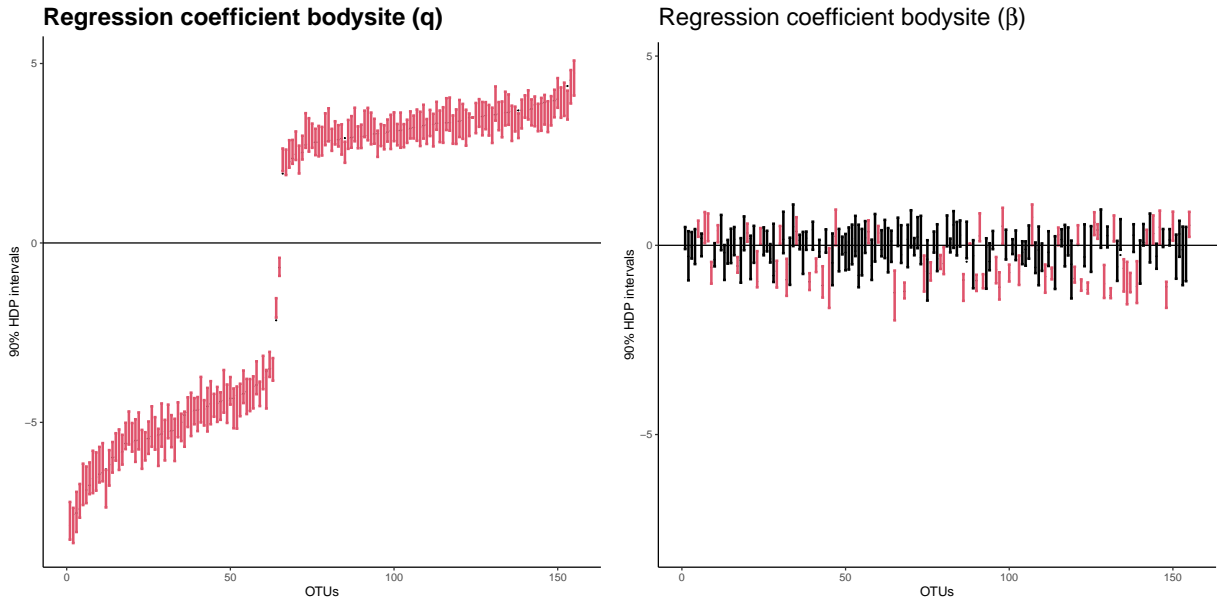


Figure 6: 90% HPD intervals of the θ (left) and γ (right) regression parameter corresponding to the body site covariate, sorted according to the median of the θ regression coefficient across the posterior samples. Intervals that do not contain the zero are coloured in red.

4.2 Bayesian structural learning of gut microbiota

We now turn to the main objective of the analysis, that of recovering the underlying network of dependencies between the OTUs. The space of possible graphs among 155 nodes is huge, creating a statistical and computational challenge at a level that has not been considered before in the context of Bayesian structural learning. Thus a few checks and considerations were made. Firstly, we start the MCMC chain by setting the initial graph to the graph detected by rMAGMA using zero-inflated negative Binomial as marginals (Cougoul et al., 2019) and the stability selection criterion **stars** for model selection (Liu et al., 2010). Secondly, we perform the structural learning for a long number of iterations, namely 10 million MCMC iterations, making use of a high performance computing cluster. Thirdly, we run five parallel chains, in order to check if there is convergence to similar graphs. We also check the sensitivity to the graph prior, by setting the edge probability π to 0.04 (i.e. a high sparsity, at the level of the initial graph detected by rMAGMA) for two of the chains and the default value of 0.5 for the other three. Overall, we observe very high correlations among the edge posterior probabilities from four of the chains, ranging between 0.97 and 1, and lower but still high correlations with the fifth one, with values ranging between 0.68 and 0.7. For the rest of the analysis, we consider the chain that resulted in the highest log-likelihood when evaluated at the posterior estimates of the marginal distributions and precision matrix.

Setting a cutoff of 0.5 on the edge posterior probabilities, the network contains 352 edges. Figure 7 shows the overlap between these edges and the optimal graph detected by rMAGMA (Cougoul et al., 2019). There is a moderate overlap, which is reassuring as the two methods share many common features. A major advantage of DWGM, which has not

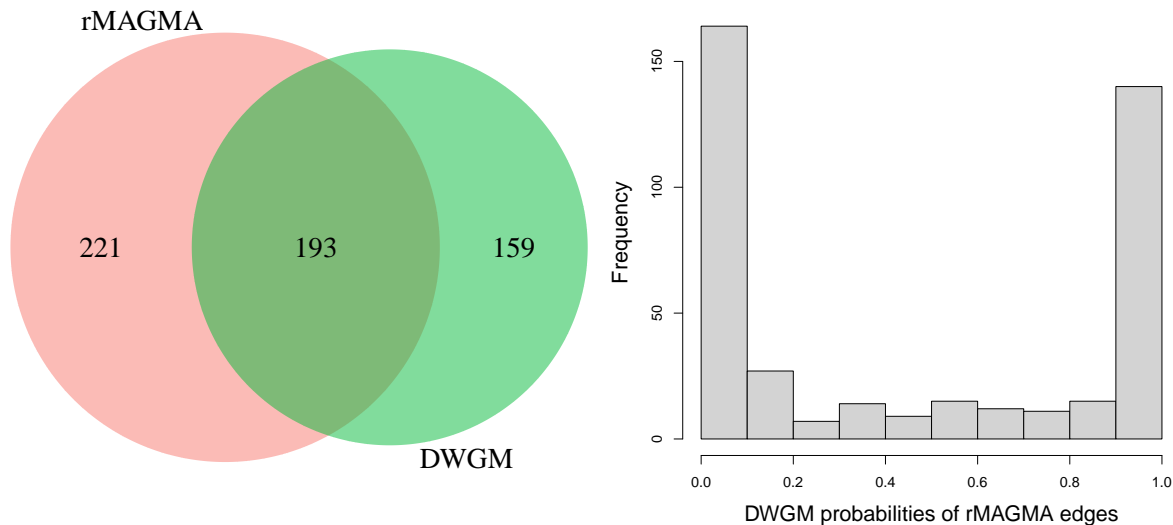


Figure 7: Left: Venn diagram comparing the optimal graph detected by rMAGMA using the **stars** criterion and the optimal graph obtained by DWGM by setting a cutoff of 0.5 on the posterior edge probabilities. Right: Histogram of DWGM posterior edge probabilities associated to the edges detected by rMAGMA.

been used before in the context of microbiome analyses, is that the uncertainty around the optimal graph is also measured. This is particularly important for structural learning in high dimensions. Indeed, the right plot of Figure 7 shows how many of the edges detected by rMAGMA have a low posterior edge probability calculated by DWGM.

As a final result, we investigate the impact that the inclusion of covariates has on the inference of the underlying graph. The expectation is that unaccounting for potential differences between the two environmental sites will lead to the detection of spurious interactions (Vinciotti et al., 2016; Cougoul et al., 2019). To this end, we compare our proposed approach with a Gaussian copula graphical model that uses the empirical distribution for the marginals (GCGM), i.e. a model that does not make use of covariate information. We run also GCGM using 10 million iterations for the structural learning part and using the same prior on the graph ($\pi = 0.04$). Figure 8 shows how the posterior distribution on graph sizes from the DWGM model (left) is concentrated on a sparser graph compared with the posterior distribution from the GCGM model, suggesting the possibility of spurious links being detected by this second analysis where covariates have been omitted. As a side effect, GCGM has also a much higher computational time (224 hours versus 124 hours for DWGM on the same cluster), since the computational time of the methods is correlated with the sparsity level of the graphs that are sampled.

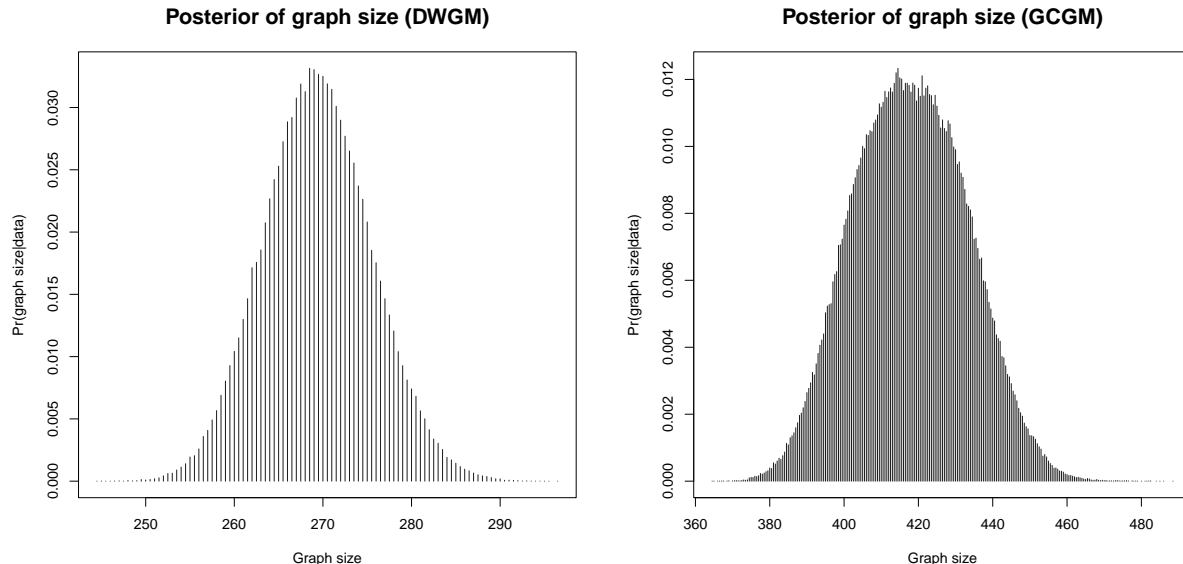


Figure 8: Posterior distribution of graph sizes for the model DWGM that accounts for covariates (left) versus the Gaussian copula graphical model that does not make use of covariates (GCGM, right).

5 Conclusion

In this paper, we have presented a copula graphical modelling approach to recover the network of interactions between microbes from high dimensional count data provided by the latest microbiome experiments. The approach has the following key features. Firstly,

it allows the inclusion of covariates in the marginal components of the model. This is useful, both in quantifying the effect of covariates of interest on microbial abundances and in aiding network recovery. Secondly, discrete Weibull regression is used for modelling the marginal distributions conditional on the covariates and is shown to be a simple yet flexible choice compared to more commonly used distributions for count data. Moreover, its definition as a discretized continuous Weibull distribution provides a latent continuous space in the vicinity of the data with a one-to-one mapping with the inferred conditional independence graph. This may be useful in deriving theoretical properties of the approach. Thirdly, a Bayesian inferential procedure based on the extended rank likelihood and on an efficient continuous-time birth-death process allows to account for the full uncertainty both in the marginals and in the graph component. The method is implemented in the R package `BDgraph`.

A simulation study and a real data analysis of microbiome data show the usefulness of the proposed approach at inferring networks from high-dimensional count data in general, and its relevance in the context of microbiota data analyses in particular.

Acknowledgment

This project was partially supported by the European Cooperation in Science and Technology (COST) [COST Action CA15109 European Cooperation for Statistics of Network Data Science (COSTNET)].

References

- Behrouzi, P. and E. Wit (2019). Detecting epistatic selection with partially observed genotype data by using copula graphical models. *Journal of the Royal Statistical Society: Series C (Applied Statistics)* 68(1), 141–160.
- Burger, D., R. Schall, J. Ferreira, and D.-G. Chen (2020). A robust Bayesian mixed effects approach for zero inflated and highly skewed longitudinal count data emanating from the zero inflated discrete Weibull distribution. *Statistics in Medicine* 39(9), 1275–1291.
- Chakraborty, S. (2015). Generating discrete analogues of continuous probability distributions - A survey of methods and constructions. *Journal of Statistical Distributions and Applications* 2(1), 1–30.
- Cougoul, A., X. Bailly, and E. Wit (2019). MAGMA: inference of sparse microbial association networks. *bioRxiv*.
- Friedman, J. and E. Alm (2012). Inferring correlation networks from genomic survey data. *PLoS Computational Biology* 8(9), e1002687.
- Friedman, J., T. Hastie, and R. Tibshirani (2008). Sparse inverse covariance estimation with the graphical lasso. *Biostatistics* 9(3), 432–441.
- Haselimashhadi, H., V. Vinciotti, and K. Yu (2018). A novel Bayesian regression model for counts with an application to health data. *Journal of Applied Statistics* 45(6), 1085–1105.

- HMP Consortium (2012). A framework for human microbiome research. *Nature* 486(7402), 215–221.
- Hoff, P. (2007). Extending the rank likelihood for semiparametric copula estimation. *The Annals of Applied Statistics* 1(1), 265–283.
- Klakattawi, H., V. Vinciotti, and K. Yu (2018). A simple and adaptive dispersion regression model for count data. *Entropy* 20(2), 142.
- Kurtz, Z., C. Müller, E. Miraldi, D. Littman, M. Blaser, and R. Bonneau (2015). Sparse and compositionally robust inference of microbial ecological networks. *PLoS Computational Biology* 11(5), e1004226.
- Lauritzen, S. (1996). *Graphical Models*. Clarendon Press.
- Le Chatelier, E., T. Nielsen, J. Qin, E. Prifti, F. Hildebrand, et al. (2013). Richness of human gut microbiome correlates with metabolic markers. *Nature* 500(7464), 541–546.
- Lee, K., B. Coull, A.-B. Moscicki, B. Paster, and J. Starr (2020). Bayesian variable selection for multivariate zero-inflated models: Application to microbiome count data. *Biostatistics* 21(3), 499–517.
- Lee, K., A. Thomas, A. Bolte, J. Björk, L. Kist de Ruijter, et al. (2022). Cross-cohort gut microbiome associations with immune checkpoint inhibitor response in advanced melanoma. *Nature Medicine*.
- Liu, H., J. Lafferty, and L. Wasserman (2009). The nonparanormal: Semiparametric estimation of high dimensional undirected graphs. *Journal of Machine Learning Research* 10(80), 2295–2328.
- Liu, H., K. Roeder, and L. Wasserman (2010). Stability approach to regularization selection (StARS) for high dimensional graphical models. *Neural Information Processing Systems* 24, 1432–1440.
- Mohammadi, A., F. Abegaz, E. van den Heuvel, and E. Wit (2017). Bayesian modelling of Dupuytren disease by using Gaussian copula graphical models. *Journal of the Royal Statistical Society: Series C (Applied Statistics)* 66(3), 629–645.
- Mohammadi, A. and E. Wit (2015). Bayesian structure learning in sparse Gaussian graphical models. *Bayesian Analysis* 10(1), 109–138.
- Mohammadi, R., H. Massam, and G. Letac (2021). Accelerating Bayesian structure learning in sparse Gaussian graphical models. *Journal of the American Statistical Association* 0(0), 1–14.
- Mohammadi, R. and E. Wit (2019). BDgraph: An R package for Bayesian structure learning in graphical models. *Journal of Statistical Software* 89(3), 1–30.
- Pedersen, H., V. Gudmundsdottir, H. Nielsen, T. Hyötyläinen, T. Nielsen, et al. (2016). Human gut microbes impact host serum metabolome and insulin sensitivity. *Nature* 535(7612), 376–381.

- Peluso, A., V. Vinciotti, and K. Yu (2019). Discrete Weibull generalized additive model: an application to count fertility data. *Journal of the Royal Statistical Society: Series C* 68(3), 565–583.
- Prost, V., S. Gazut, and T. Bröls (2021). A zero inflated log-normal model for inference of sparse microbial association networks. *PLOS Computational Biology* 17(6), 1–17.
- Qin, J., R. Li, J. Raes, M. Arumugam, K. Burgdorf, et al. (2010). A human gut microbial gene catalogue established by metagenomic sequencing. *Nature* 464, 59–65.
- Roverato, A. (2002). Hyper inverse Wishart distribution for non-decomposable graphs and its application to Bayesian inference for Gaussian graphical models. *Scandinavian Journal of Statistics* 29(3), 391–411.
- Roy, A. and D. Dunson (2020). Nonparametric graphical model for counts. *Journal of Machine Learning Research* 21(229), 1–21.
- Sklar, A. (1959). Fonctions de répartition à n dimensions et leurs marges. *Publications de l’Institut de Statistique de l’Université de Paris* 8, 229–231.
- Vinciotti, V., E. Wit, R. Jansen, E. Geus, B. Penninx, D. Boomsma, and P. Hoen (2016). Consistency of biological networks inferred from microarray and sequencing data. *BMC Bioinformatics* 17.
- Yang, L., E. Frees, and Z. Zhang (2020). Nonparametric estimation of copula regression models with discrete outcomes. *Journal of the American Statistical Association* 115(530), 707–720.